Macromolecules

Article

pubs.acs.org/Macromolecules

Ester Functionalization of Polypropylene via Controlled Decomposition of Benzoyl Peroxide during Solid-State Shear Pulverization

Mirian F. Diop[†] and John M. Torkelson*[,†,‡]

[†]Department of Chemical and Biological Engineering, Northwestern University, Evanston, Illinois 60208, United States

[‡]Department of Materials Science and Engineering, Northwestern University, Evanston, Illinois 60208, United States

Supporting Information

ABSTRACT: Polypropylene (PP) is a nonpolar polyolefin that is sometimes functionalized with polar molecules to allow for reactive compatibilization and improve interfacial adhesion. Functionalized PP is conventionally synthesized by melt extrusion at elevated temperature (T) (≥~180 °C) with a radical initiator and polar monomer, e.g., maleic anhydride. A drawback to high T functionalization is that β-scission, which leads to cleavage of C−C backbone bonds, is significant and results in major molecular weight (MW) reduction and property degradation. We present a novel method of functionalizing PP using benzoyl peroxide (BPO) alone by a process called solid-state shear pulverization (SSSP), resulting in ester functional groups (benzoates) grafted at high yield onto PP. Ester functionalized PP (PP-g-ES) is synthesized with limited MW reduction because SSSP is done at sufficiently low T to suppress β-scission. Characterization before and after grafting at 0.18 mol % (0.46 wt %) graft level indicates that functionalization (and subsequent purification) is accompanied by only one chain scission event per 12 400 PP repeat units, resulting in 17% and 36% reductions in number-average MW and weight-average MW, respectively. Benzoate grafting levels are tuned from 0.08 to 0.41 mol % (0.22 to 1.14 wt %) by varying the BPO feed level. In addition to limited MW reduction, PP-g-ES exhibits modified interfacial properties, the ability to undergo transesterification reactions consistent with reactive compatibilization, and little to no loss of physical and mechanical properties relative to neat PP.

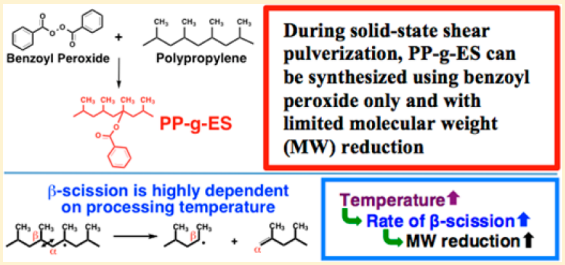

INTRODUCTION

Polyolefins are nonpolar by nature which leads to excellent chemical resistance but poor compatibility with polar molecules. When functionalized with polar moieties[1−15] such as hydroxyl groups,[2,3] itaconates,[4] methacrylate esters,[4,5] and maleic anhydride,[6−12] the modified polyolefins are useful as compatibilizers in blends,[16−18] composites,[19,20] and nanocomposites.[21−23] Commercial, functionalized polyolefins are based on covalent addition of functional monomers to polyolefins in the presence of a radical initiator; the major categories of this type of functionalization are discussed in detail in a recent publication.[12] The most common method used for functionalization is melt extrusion; under the high temperature (T) conditions utilized, functionalization is usually accompanied by undesirable side effects, including chain scission, branching, and cross-linking.[24−28] For this reason, there is ongoing interest to develop improved, commercially scalable methods for postpolymerization functionalization of polyolefins in the presence of both a radical initiator, such as an organic peroxide, and a functional monomer.[12]

An alternative method for direct functionalization of polyolefins in the absence of functional monomer was described in a 2005 review by Boaen and Hillmyer,[29] who stated, "An interesting approach that is related but could prove to be more efficient is the direct functionalization with organic peroxides alone." Attempts to achieve direct functionalization have been limited to the use of asymmetric peroxy derivatives (e.g., acrylic peroxides, peroxyesters, and peroxyketals) that possess an extra functional group (e.g., ester, ketone, carboxylic acid) in addition to the peroxidic O−O bond.[30−37] Following the seminal work by DeNicola et al.[30] in 1995 on direct functionalization of polyolefins using unsaturated peroxides and concluding in 2005, several studies were published regarding polyolefin functionalization with peroxy derivatives.[31−37] These studies mostly relied on thermal decomposition of a peroxy derivative to functionalize a polyolefin at or above the melt T of the polyolefin.

The generalized mechanism for direct functionalization with a peroxyester (see Scheme 1) begins with the dissociation of an asymmetric peroxyester (R′O−OCOR″−X) into two radicals, R′O$^\bullet$ and $^\bullet$OCOR″−X, with R′O$^\bullet$, an alkoxy radical, being the more reactive of the two radicals formed (Scheme 1, step 1). The asymmetric peroxide is chosen so that it decomposes to form a less reactive radical, $^\bullet$OCOR″−X, with X being a

Received: August 2, 2013
Revised: September 5, 2013
Published: September 17, 2013

   dx.doi.org/10.1021/ma401628u | Macromolecules 2013, 46, 7834−7844

Scheme 1. Generalized Mechanism for Direct Functionalization of a Polyolefin with a Peroxy Derivative

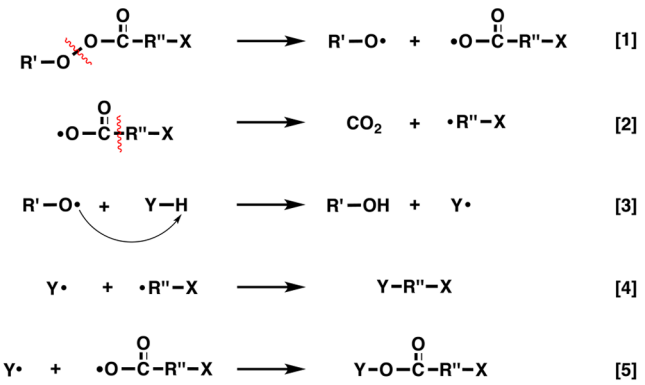

X = hydrogen or functional groups such as carboxylic acids, esters, or ketones
Y−H = polyolefin, e.g., polyethylene, polypropylene

carbonyl functional group (e.g., carboxylic acid, ester, or ketone). During processing, •OCOR″−X undergoes decarboxylation to produce •R″−X (Scheme 1, step 2). The alkoxy radical, R′O•, can participate in chain transfer with the polyolefin (Y−H) to produce a macroradical (Scheme 1, step 3). The polyolefin macroradical (Y•) then terminates with •R″−X to form a functionalized polyolefin. Acrylic peroxides and peroxyketals undergo slightly more complicated mechanisms that include peroxide decomposition induced by polyolefin macroradicals and rearrangements of radicals resulting in polyolefins functionalized with esters, carboxylic acids, or epoxides.[31,32,34,36]

In the late 1990s, Assoun et al.[37] studied polypropylene (PP) carboxylation with peroxy derivatives by melt extrusion at 180 °C in an inert environment. They investigated the effect of the chemical structure of peroxy derivatives on grafting degree, β-scission, and branching. β-scission is highly T dependent and occurs as a result of rearrangement of a PP macroradical into two chains: one with a terminal double bond and the other with a terminal radical.[24] They determined that even though a highly reactive R′O• radical (Scheme 1) could improve grafting efficiency, up to ∼17%, it resulted in major molecular weight (MW) reduction as a result of β-scission. They also found that the presence of a double bond in the •OCOR″−X radical could lead to branch and/or cross-link formation.

From 2000 to 2005, Maillard and co-workers[31−36] published extensively on direct functionalization of polyethylene (PE) and PP using asymmetric peroxy derivatives, e.g., acrylic peroxides, peroxyesters, peroxyketals, and unsaturated peroxides. Using a 2.5 h batch process in an inert environment at 160 °C and atmospheric pressure, they achieved ester functionalization of PE with peroxyesters and peroxyketals.[31−33] In addition to functionalizing PE, they observed varying degrees of cross-linking depending on the nature of the radicals formed after peroxide decomposition. They also showed that functionalization of isotactic and atactic PP was possible using peroxyesters or peroxyketals and a 160 °C batch process.[34,35] Although they expected greater functionalization of PP relative to PE because the C−H bond dissociation energies are lower for methane hydrogens than for methyl or methylene hydrogens, they found that hydrogen abstraction (needed for functionalization) "hardly occurs"[34] with PP and inferred that PP methyl groups hinder hydrogen abstraction by 1,1-dimethylethoxy radicals.[34]

Maillard and co-workers[31−36] and Assoun et al.[37] acknowledged the possibility of achieving direct functionalization with an acyloxy radical, •OCOR″−X, i.e., without undergoing decarboxylation to form an alkyl radical, •R″−X. Indeed, this type of termination reaction is possible as long as the alkyl radical is more stable than its acyloxy counterpart.[38,39] The tendency of an acyloxy radical to undergo decarboxylation depends on T, pressure, and the stability of the alkyl radical that is formed.[38,39] For most diacyl peroxides, decarboxylation happens almost simultaneously with the cleavage of the O−O bond at all T's; this is not so for diacetyl peroxide or benzoyl peroxide (BPO), which both form unstable alkyl radicals (methyl and phenyl, respectively) after decarboxylation.[38] Additionally, the presence of a double bond stabilizes an acyloxy radical and reduces the rate of decarboxylation.[37] It is under one of these conditions (i.e., the formation of radicals from unsaturated asymmetric peroxides) that Assoun et al.[37] obtained data that suggested that small levels of direct functionalization of PP with esters from acyloxy radicals (•OCOR″−X in Scheme 1) had been achieved. Chateauneuf et al.[40] demonstrated that for benzoyloxy radicals formed from BPO decomposition the rate constant for decarboxylation depends strongly on T, increasing by ∼200-fold as T increases from 25 to 200 °C. Thus, a potential approach for increasing the grafting degree of acyloxy radicals (in particular, benzoyloxy radicals) during polyolefin functionalization is to decrease the processing T. By so doing, the extent of β-scission, and thus MW reduction, can be decreased as well.

Here, we show for the first time that a symmetric organic peroxide, BPO, can be used in the absence of a polar monomer to graft polar functional groups onto PP. In particular, we demonstrate that solid-state shear pulverization (SSSP), a low T, continuous process with potential for high throughput, provides a tunable route to synthesize ester functionalized PP (PP-g-ES). This process uses a twin-screw melt extruder modified with a cooling system to maintain the polymer in the solid state.[12,41−50] Solid-state shear pulverization is accompanied by high shear stresses and compressional forces that cause repeated fragmentation and fusion of material; conditions are tuned by feed rate, screw speed, screw design, and T.[42] In addition to being solventless, SSSP is industrially scalable. (Polyolefins have been processed by SSSP with a commercial-scale apparatus at rates exceeding 150 kg/h.) Compatibilization and intimate mixing of immiscible blends[43−46] and effective dispersion and exfoliation in composites and nanocomposites can result from SSSP.[47−51] Very recently, we also showed that SSSP can be used to synthesize maleic anhydride grafted PP with strongly suppressed MW reduction.[12] In the present study, by using SSSP for postpolymerization synthesis of PP-g-ES, we present a platform of low-T chemistries that is unattainable with high-T melt processing. The functionalization results in benzoate side groups that can modify interfacial interactions with polar molecules and result in a reactive PP of the type useful in reactive compatibilization.

■ EXPERIMENTAL SECTION

Materials. Polypropylene (Total Petrochemicals; MFI = 1.5 g/10 min; ASTM standard D-1238 at 230 °C/2160 g load; reported by the supplier) was used as received. Benzoyl peroxide was used as received (SigmaAldrich). Xylene, octadecyl acrylate (ODA), and 1-pyreneacetic acid (Pyr-AA) were used for characterizing grafting degrees and reactivity of the PP-g-ES and were used as received (SigmaAldrich). A

dx.doi.org/10.1021/ma401628u | Macromolecules 2013, 46, 7834−7844

Table 1. Variables for Sample Composition, Processing Method, and Characterization of Benzoate Grafting Degrees, Crystallinity, and Tensile Properties for Neat PP and PP-*g*-ES Samples Made via SSSP

sample	amount of BPO Added (wt %)	processing method	grafting degree[a] (wt %)	grafting degree[a] (mol %)[b]	grafting yield (%)	crystallinity (%)	Young's modulus (MPa)	yield strength (MPa)
neat PP pellets (as received)						45	1250 ± 80	36 ± 1
neat PP (after SSSP)		SSSP				44	1170 ± 60	35 ± 1
PP-*g*-ES/1	0.5	SSSP	0.22	0.08	87	41	1270 ± 30	36 ± 1
PP-*g*-ES/2	1.0	SSSP	0.33	0.12	65	42	1190 ± 30	34 ± 1
PP-*g*-ES/3	1.5	SSSP	0.46	0.18	61	41	1130 ± 30	32 ± 1
PP-*g*-ES/4	3.0	SSSP	0.81	0.30	52	42	1190 ± 60	32 ± 2
PP-*g*-ES/5	6.0	SSSP	1.14	0.41	36	40	1080 ± 40	29 ± 1
PP-*g*-ES/4MM	3.0	melt mixing						

[a]Grafting degree can also be expressed in μequiv (i.e., μmol of benzoates in 1 g of PP-*g*-ES) by simple stoichiometric calculations (e.g., 0.18 wt% is equivalent to 0.22 μequiv benzoate grafted onto PP). [b]Functionalization in mol % represents the number of moles of benzoates per mole of repeat units multiplied by 100%.

phenolic antioxidant, Songnox 6260 (Songwon), was used as received in samples made for rheological characterization.

Synthesis of PP-*g*-ES with SSSP. The PP and BPO were pulverized using a relatively harsh screw design[42] at 200 rpm screw speed and 100 g/h feed rate. The pulverizer was a pilot-plant/research scale Berstoff twin-screw extruder (screw diameter = 25 mm, length/diameter = 26.5) modified with a cooling system (a Budzar Industries WC-3 chiller operating at −6 °C); the same apparatus was used in previous SSSP studies.[12,41−50] (It should be noted that the *T* of the solid-state polymer in the pulverizer may, at various locations, exceed room temperature by several tens of degrees and be warm to the touch upon exiting the pulverizer.) Samples of PP-*g*-ES were prepared by SSSP using 0.5−6.0 wt % BPO in the feed. A PP-*g*-ES sample prepared with 3 wt % BPO was also prepared by melt processing for 10 min at 200 °C with an Atlas Electronic Devices MiniMAX molder (cup-and-rotor mixer) at maximum rotor speed and with three steel balls in the cup to provide chaotic mixing.[52] Table 1 shows sample composition and process methods.

Purification of PP-*g*-ES. To ensure high purity and the absence of contaminants, PP-*g*-ES samples employed for quantification of carbonyl grafting, contact angle measurements, and demonstration of reactivity were purified to remove unreacted BPO by dissolution in boiling xylene followed by precipitation with methanol. The samples were dried under vacuum at 70 °C for 24 h. The PP-*g*-ES samples for rheology were purified using a variety of methods that combined washing with acetone and annealing under vacuum; samples were annealed either at room *T* for 96 h or at 50 °C for 48 h. For each annealing condition, two sets of samples were studied: one set was washed with acetone before annealing, and the other was not washed before annealing. For the washing step, 100 g of PP-*g*-ES was stirred in 300 mL of acetone for 3 h at room *T*; the PP-*g*-ES was then removed by filtration. The PP-*g*-ES samples used in high-*T* gel permeation chromatography (high-*T* GPC) and physical and mechanical property characterization were purified by washing with acetone and annealing at 50 °C for 48 h.

Quantification of Carbonyl Grafting. In order to create a calibration curve, ODA/PP blends were prepared by melt processing at 200 °C in a MiniMAX molder for 10 min and at maximum rotor speed with three steel balls in the cup in order to provide chaotic mixing.[52] Blend products were compression molded into thin films (∼0.3 mm thick) for Fourier transform infrared (FTIR) spectroscopy using a PHI hot press coupled with a PHI cold press. Octadecyl acetate was chosen because of its structural similarity to PP-*g*-ES. For each blend, three sets of FTIR data were collected with 64 scans and 4 cm^{-1} resolution. Purified PP-*g*-ES samples were compression molded into thin films (∼0.3 mm thick) and tested under the same conditions as ODA/PP blends.

Rheological Measurements. Neat PP and PP-*g*-ES samples were tested with 0.5 wt % Songnox 6260 added to each sample to prevent thermal degradation. Samples were compression molded into disks devoid of bubbles using PHI presses. Small-amplitude oscillatory shear data were collected at 180 °C, with 2% strain over a frequency range of 0.01−100 rad/s (measuring from high to low frequency), using a strain-controlled Rheometrics Scientific ARES rheometer equipped with 25 mm parallel plates.

Physical and Mechanical Properties. Thermal analysis employed a Mettler Toledo differential scanning calorimeter (DSC 822e). Samples were heated at 40 °C/min to 200 °C, held at 200 °C for 5 min, cooled at 40 °C/min to 40 °C, held at 40 °C for 3 min, heated at 10 °C/min to 200 °C, held at 200 °C for 5 min, and cooled at 10 °C/min to 40 °C. The crystallinity was determined from the final cooling step.

Films with ∼0.7 mm thickness were prepared by pressing in a PHI hot press at 200 °C for 5 min and then rapidly cooling in a PHI cold press for 15 min. Tensile specimens were prepared according to ASTM D1708; dumbbell-shaped specimens were cut from films using a Dewes-Gumbs die. An MTS Sintech 20/G (100 kN load cell; crosshead speed = 5 cm/min) was used to obtain Young's modulus and yield strength values at room temperature.

Contact Angle Measurement. Neat PP and PP-*g*-ES samples were compression molded into thin films (∼0.3 mm thick) with smooth surfaces using a PHI hot press at 200 °C for 5 min and then rapidly cooling in a PHI cold press for 10 min. The static contact angle of a droplet of deionized water (5 μL) on the surface of each disk was determined using a KRUS drop shape analysis system, DSA 100; results for each sample were averaged over 20 measurements. Reported values of contact angle measurements have ±1° experimental errors.

Demonstration of Reactivity of PP-*g*-ES with Pyr-AA. 10 g/L PP-*g*-ES samples were dissolved in 0.30 g/L solutions of Pyr-AA in xylene. Solutions were held at 130 °C for 4 h, after which PP-*g*-ES was precipitated with methanol. To remove unreacted Pyr-AA, samples were purified six times by dissolution in boiling xylene and precipitation in methanol. Pyrene label fluorescence was measured with a Photon Technology International fluorimeter (λ_{exc} = 344 nm).

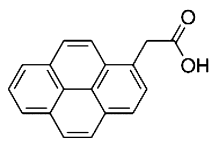

1-pyreneacetic acid (Pyr-AA)

RESULTS AND DISCUSSION

Quantitative Characterization of Ester Functionalization Levels on PP-*g*-ES: FTIR Spectroscopy. Figure 1

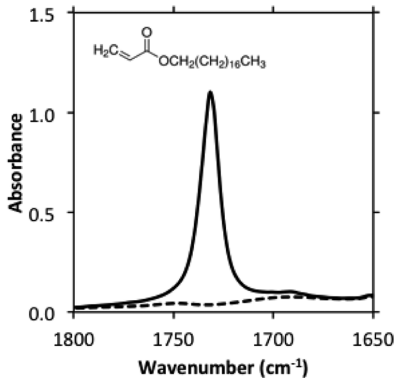

Figure 1. FTIR spectra of an ODA/PP blend containing 155 μequiv of ODA, i.e., 5 wt % ODA in ODA/PP blend (solid curve) and neat PP (dashed curve). The inserted molecular structure is that of octadecyl acrylate (ODA).

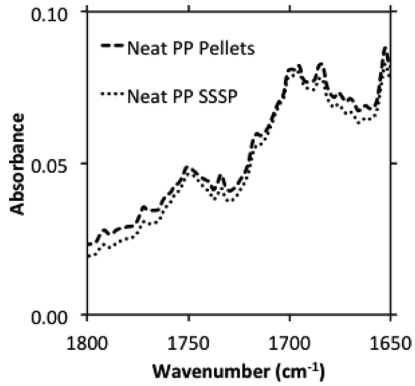

Figure 2. FTIR spectra of neat PP as received (dashed curve) and neat PP after SSSP (dotted curve).

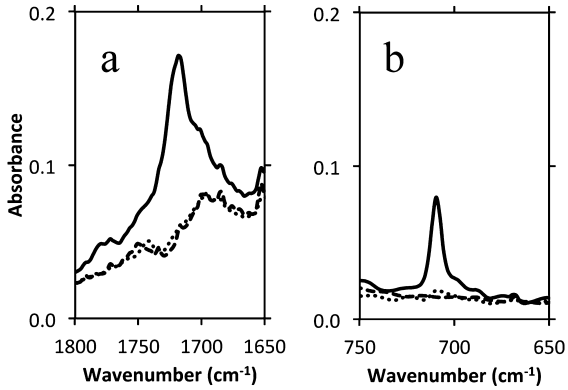

Figure 3. FTIR spectra of PP-*g*-ES/4 (solid curve), PP-*g*-ES/4MM (dotted curve), and neat PP as received (dashed curve) in spectral ranges of (a) 1800−1650 and (b) 750−650 cm^{-1}.

compares FTIR spectra of neat, as-received PP and a sample containing 5.0 wt % ODA in an ODA/PP blend. The peak at 1732 cm^{-1} is present only for the ODA/PP blend and is associated with the ODA ester functional group.[53] The inset in Figure 1 is the chemical structure of ODA. A peak at 841 cm^{-1}, specific to PP and absent for BPO, is used for normalization of each sample spectrum. For spectral analyses, the data between 1800 and 1600 cm^{-1} and between 930 and 740 cm^{-1} were deconvoluted into component peaks using a Lorentzian function. This yielded accurate peak intensities while accounting for peak overlaps and inconsistent baselines between spectra. A calibration curve based on ODA was determined using

$$[\text{ester}] = 0.25(A_{1732}/A_{841}) \quad (1)$$

where [ester] is the grafting degree and measured in mol % (i.e., moles of benzoate per mole of PP repeat unit) and A_{1732} and A_{841} are the areas under the peaks at 1732 and 841 cm^{-1}, respectively. The grafting yield was calculated using

$$\text{grafting yield} = ([\text{ester}]/[\text{BPO}]_0) \times 100\% \quad (2)$$

where [ester] is as defined in eq 1 and $[\text{BPO}]_0$ is the initial amount of BPO added during SSSP; both variables were measured in mol %. (It must be noted that if each of the two benzoyloxy radicals resulting from the dissociation of BPO were to be grafted to PP, then the grafting yield would be 200%. Of course, for this to occur, all PP radicals would have to be generated solely by chain scission accompanying SSSP, without any chain transfer reactions. Chain scission has been shown to accompany SSSP of PP, albeit at quite limited levels, under harsh pulverization conditions and decreasing with decreasing levels of work done on the PP during SSSP.[42,43]) Grafting degrees and yields of PP-*g*-ES samples were determined using eqs 1 and 2 and are reported in Table 1; grafting degrees are presented in both mol % and wt %.

Figure 2 compares the FTIR spectra for neat, as-received PP, and neat PP after SSSP. Because of the strong similarity between the spectra in the regions of interest (1800−1600 cm^{-1}), we can conclude that no functionalization due to ketonization or carboxylic acid formation (as a result of radical stabilization by atmospheric oxygen[54]) occurs during SSSP processing of neat PP. Figure 3 compares the FTIR spectra of PP-*g*-ES/4, PP-*g*-ES/4MM, and neat PP pellets and confirms the presence of a strong absorbance peak for PP-*g*-ES/4 at 1720 cm^{-1} and the absence of this absorption for the melt processed sample (see Figure 3a). As explained above, this peak is associated with ester functional groups; the slight shift of this peak to a lower wavenumber (as compared to the ester peak observed for ODA) is expected for aromatic esters.[53] In Figure 3b, we see an absorbance at ∼740 cm^{-1} for PP-*g*-ES/4. This absorbance is associated with phenyl group attachment to the PP backbone and is absent for PP-*g*-ES/4MM, which confirms that no significant functionalization of an ester or addition of a phenyl group can be achieved using BPO via high-T melt processing. The absence of functionalization during melt processing can be understood from the T dependence of BPO dissociation into radicals.[40,55] A detailed explanation for this is given in the next subsection.

As compared to grafting yields reported for PP-*g*-ES synthesized with peroxyesters[34,37] and unsaturated peroxides[35] at 160−180 °C and in an inert environment, the 36−87% grafting yields (corresponding to 0.41−0.18 mol % grafting degrees, respectively) obtained during PP-*g*-ES synthesis via SSSP in an air environment are significantly higher. Assoun et al.[37] reported ∼17% (and 0.02 mol %) as the largest grafting yield for a series of peroxyesters used for PP functionalization by melt extrusion at 180 °C and in an N_2 environment. Saule et al.[34] reported a grafting yield of 5% for isotactic PP grafted in a 2.5 h batch process carried out in an inert environment at 160 °C using a peroxyester. For a series of unsaturated peroxides, which were expected to significantly improve grafting yields in PP, Saule et al.[35] reported a maximum grafting yield of ∼40%.[56] It is evident from these comparisons that PP-*g*-ES synthesis

dx.doi.org/10.1021/ma401628u | Macromolecules 2013, 46, 7834−7844

from BPO via SSSP results in improvement in both grafting degree and grafting yield over the PP-*g*-ES counterparts that were prepared at elevated *T* using asymmetric peroxyesters.

A combination of factors may contribute to the high grafting yields obtained with SSSP-based synthesis of PP-*g*-ES. During SSSP, the solid-state materials are exposed to high shear stresses and compressive forces. Such stresses and forces have previously been shown to yield unprecedented levels of debundling, exfoliation, and dispersion of highly agglomerated and entangled carbon nanotubes, graphite (layered sheets of graphene), and even rice husk ash during SSSP processing of PP composites and nanocomposites.[47−51] Substantial levels of friction accompany SSSP of polymers, resulting in a *T* rise of the solid-state material in the pulverizer, which for the PP/BPO system can lead to thermal decomposition of some of the BPO. Such stresses and forces accompanying SSSP have also been shown to yield tunable, low levels of chain scission,[42] leading via combination reactions of polymeric radicals to the mechanochemical formation of block copolymers at interfacial regions of immiscible polymer blends.[44,46] Mechanical forces and stresses have been shown in other research to lead to mechanochemistry involving small molecules in polymers as well as mechanophores covalently attached to polymers.[57−60] Thus, some BPO dissociation into benzoyloxy radicals during SSSP of the PP/BPO system may be mechanochemically based and even be enhanced by the interplay of thermal and mechanical effects. Further study is warranted, especially to determine whether SSSP may allow for commercial-scale application of mechanochemistry to polymeric materials.

Proposed Mechanism for Benzoate Functionalization of PP during SSSP. On the basis of the FTIR results, we propose the mechanism presented in Scheme 2 for the addition of benzoyloxy radicals to PP backbone during SSSP. The functionalization begins with the decomposition of BPO into benzoyloxy radicals (Scheme 2, step 1). Because of the low-*T* conditions, the rate of decarboxylation (Scheme 2, step 2) during SSSP is very low,[40] allowing for the presence of benzoyloxy radicals in large excess of phenyl radicals. A benzoyloxy radical can abstract a hydrogen from a PP chain to form a PP macroradical (Scheme 2, step 3). Reaction between a PP macroradical and a benzoyloxy radical results in PP functionalization with a benzoate (Scheme 2, step 4). The presence of phenyl groups (occurring as a result of benzoate functionalization) is supported by the presence of the peak at ~740 cm^{-1} (see Figure 3b).

Unlike processing via SSSP, melt processing of PP and BPO does not result in benzoate functionalization of PP. Even before the PP melts[55,61] in the melt processing study, the BPO totally decomposes and its radicals are lost as a result of termination reactions with each other and subsequent production of inert molecules;[62] it is for this reason that BPO is not used as radical initiator in conventional PP functionalization. Additionally, BPO decomposition during melt processing results in the production of phenyl radicals in large excess of benzoyloxy radicals due to the increased rate of decarboxylation at the high *T* (Scheme 2, step 2).[40] Phenyl radicals produced during melt processing can abstract a hydrogen from the PP backbone to form a PP macroradical. At best, these phenyl radicals could undergo termination reactions with PP macroradicals. However, we see no indication of this type of functionalization from FTIR spectra (see Figure 3b); i.e., there is no absorbance as a result of phenyl ring addition to the PP backbone for PP-*g*-ES/4MM. Thus, by taking advantage of unique radical chemistries

Scheme 2. Proposed Mechanism for Ester Functionalization of PP Using BPO[a]

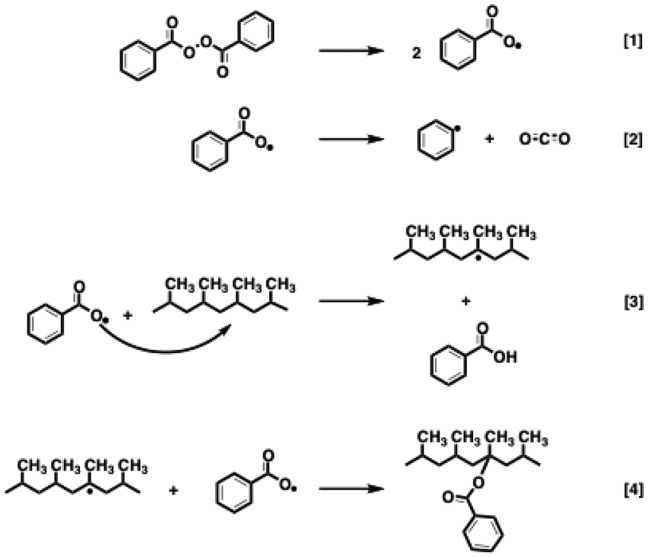

[a]During SSSP the rate of decarboxylation (see step 2) is significantly suppressed, resulting in a higher prevalence of benzoyloxy radicals formed in step 1 and allowing for the grafting of PP with benzoates. However, during melt processing, the rate of decarboxylation is high, resulting in a higher prevalence of phenyl radicals and subsequently no grafting of PP with benzoates. (In the absence of step 2, which should be negligible at the SSSP *T* conditions, the theoretical limiting yield of grafted benzoate is 100% with this scheme and the definition given in eq 2.)

afforded by the near-ambient *T* processing conditions during SSSP, we are able to achieve direct ester functionalization of PP in a way that is unattainable by conventional melt processing. (In the context of synthesis by SSSP, near-ambient *T* can mean that solid-state PP is at temperatures a few tens of degrees above room *T* but far below the melt transition of PP.)

PP-*g*-ES MW Reduction as a Function of BPO Purification Method: Rheology Characterization. A long-standing challenge associated with direct polyolefin functionalization with peroxy derivatives[30−37] or polar monomers such as maleic anhydride[6−12,24−28] is the occurrence of undesirable side reactions such as chain scission, branching, and cross-linking.[24−28] Of particular interest during PP functionalization is the occurrence of *β*-scission, which results in MW reduction of the synthesized polar PP relative to the neat PP from which it was made (see Scheme 3). The rate of *β*-scission is highly *T* dependent, increasing by 8 orders of magnitude as *T* increases from 25 to 200 °C.[24,63] The likelihood of *β*-scission raises major concern during direct ester functionalization of PP

Scheme 3. Mechanism for *β*-Scission

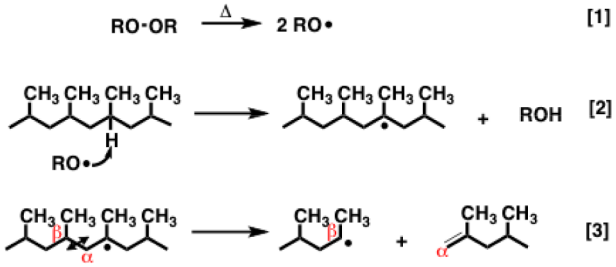

dx.doi.org/10.1021/ma401628u | Macromolecules 2013, 46, 7834−7844

via melt processing because peroxy derivatives are chosen so that their radicals are very good at abstracting hydrogen atoms from the PP backbone to form PP macroradicals. At melt-state T, PP macroradicals have a high propensity to undergo β-scission. Thus, postpolymerization functionalization of PP by melt processing results in dramatic MW reduction. For example, for PP-g-ES samples made by melt processing with asymmetric peroxy derivatives, Saule et al.[35] reported weight-average MW (M_w) reductions of 53−70% with grafting yields of 30−40%,[56] and Assoun et al.[37] reported a 24% reduction in M_w at only 0.02 mol % grafting level and ∼17% grafting yield. (Grafting yields have a maximum of 100% when grafting is done with asymmetric peroxy molecules.) Here, using rheology, we evaluate the change in PP M_w caused by benzoate functionalization and consider the effect of the method used to purify the PP-g-ES of unreacted BPO and its byproducts.

During SSSP, shear stresses and compressional forces cause repeated fragmentation and fusion of the material in the solid state.[42] Thus, we expect that unreacted BPO will be located not only on the surface of PP powder particles but also trapped within the particles. The products of SSSP processing of PP with BPO, resulting in 0.08−0.41 mol % ester functionalization and grafting yields as high as 87%, were purified of unreacted BPO and its byproducts in a number of ways prior to characterization by rheology: no purification; annealing samples under vacuum at room temperature for 96 h to purify by sublimation;[64−67] washing with acetone to remove surface BPO and then annealing under vacuum at room temperature for 96 h; annealing samples under vacuum at 50 °C for 48 h to purify by decomposition and/or sublimation;[55,64−67] and washing with acetone to remove surface BPO and then annealing under vacuum at 50 °C for 48 h.

Figure 4 compares the magnitudes of complex viscosity ($|\eta^*|$) of PP-g-ES/1, PP-g-ES/2, and PP-g-ES/3 that were

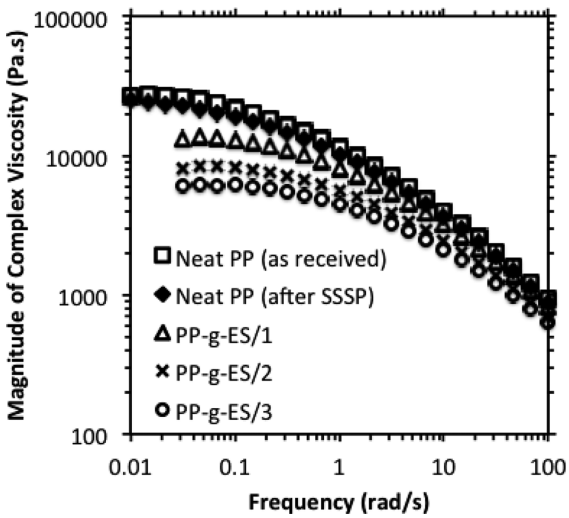

Figure 4. Magnitude of complex viscosity as a function of frequency for as-received neat PP pellet (□), neat PP pulverized (◆), PP-g-ES/1 (△), PP-g-ES/2 (×), and PP-g-ES/3 (○). Data were collected at 180 °C.

washed with acetone and annealed under vacuum at 50 °C for 48 h to those of control samples. The three PP-g-ES samples as well as the control samples exhibited $|\eta^*|$ values that were independent of frequency at low frequency. With such behavior and application of the Cox−Merz rule,[68] which relates linear viscoelastic properties to steady shear viscosity, and the Cross model,[69] it is possible to determine the zero shear rate viscosity (η_0) from $|\eta^*|$ data. Assuming that η_0 scales with M_w to the 3.4 power,[70−73] we can then use rheology to characterize the effect of SSSP processing, functionalization, and post-SSSP purification method on M_w.

Before discussing such characterization of M_w in detail, it is important to note that some samples did not exhibit the presence of a η_0 regime in the rheology data. Instead, even at the lowest frequency, $|\eta^*|$ was increasing with decreasing frequency. (Selected examples of this behavior are shown in the Supporting Information.) This behavior is believed to be associated with long-chain branching. Examples fall into two classes: (1) PP-g-ES/2 and PP-g-ES/3 that were not subjected to any purification prior to rheological testing and (2) PP-g-ES/4 and PP-g-ES/5 that were subjected to all levels of purification, which indicates that these samples, with the highest ester functionalization levels, were branched coming out of the SSSP apparatus. This branching behavior will be addressed in more detail in future work.

Neat PP after SSSP had η_0 that was 10% lower than that of neat PP pellets (i.e., η_0 = 28,500 Pa·s for neat PP after SSSP), indicating a 3% reduction in M_w. Thus, in the absence of BPO, SSSP causes nearly negligible MW reduction of neat PP. For PP-g-ES/1 (0.08 mol % graft level and 87% grafting efficiency) that was characterized directly as the output from the pulverizer without any purification step to remove unreacted BPO, η_0 was reduced by ∼61% relative to neat PP pellets, indicating a 24% reduction in M_w. This M_w reduction is similar to the 24% reduction measured by Assoun et al.[37] for a PP-g-ES sample made by melt processing and asymmetric peroxy molecules which had only 0.02 mol % functionalization, one-fourth that of our PP-g-ES/1 sample. When the same PP-g-ES/1 sample was subjected to various purification steps, the apparent reductions in M_w from zero shear rate viscosity data were 11−12% (unwashed or washed with acetone, followed by room temperature annealing under vacuum for 96 h) and 20−21% (unwashed or washed with acetone, followed by annealing at 50 °C under vacuum for 48 h). The results indicate that at low functionalization levels only very small amounts of β-scission leading to MW reduction occur during SSSP; this is also true even during post-SSSP annealing or processing under conditions that would lead to decomposition of unreacted BPO into radicals (i.e., annealing at 50 °C).

At moderate functionalization, PP-g-ES/2 and PP-g-ES/3 with 0.12−0.18 mol % ester, which require higher BPO levels in the feed, linear chain behavior is evident from rheology for all purification conditions except no purification. This implies that the PP-g-ES output from the pulverizer is linear in nature and only becomes branched if substantial levels of covalently attached benzoates and undecomposed BPO are present in the sample at the time it is subjected to melt processing. Based on η_0 values, M_w was reduced relative to neat PP by 23−25% and 27−28% in PP-g-ES/2 and PP-g-ES/3 for samples (washed with acetone or unwashed and) annealed at room temperature under vacuum for 96 h and by 30% and 36% in PP-g-ES/2 and PP-g-ES/3 for samples (washed with acetone or unwashed and) annealed at 50 °C under vacuum for 48 h. While these values of M_w reduction are not negligible, they are far below the 53−70% reductions reported by Saule et al.,[35] who did postpolymerization ester functionalization of PP by melt processing with asymmetric peroxy molecules.

dx.doi.org/10.1021/ma401628u | Macromolecules 2013, 46, 7834−7844

Table 2. MW Characterization before and after Functionalization via SSSP Using Oscillatory Shear Rheology and High-*T* GPC

		rheology		high-*T* GPC					
sample	grafting deg (mol %)	η_0 (Pa·s)	M_w reduction[a] (%)	M_n (g/mol)	M_n reduction (%)	M_w (g/mol)	M_w reduction (%)	z_c	ester groups per chain
neat PP pellets (as-received)		31 800		115 000		585 300			
PP-*g*-ES/1	0.08	14 800	20	104 900	9	439 800	25	0.10	2
PP-*g*-ES/2	0.12	9 900	29	104 400	9	422 800	28	0.10	3
PP-*g*-ES/3	0.18	7 100	36	95 400	17	376 000	36	0.21	4

[a]Percent reduction in M_w relative to neat PP pellets (as received) was calculated using the assumption that η_0 scales with M_w to the 3.4 power.

High-*T* GPC Characterization of PP-*g*-ES and Chain Scission Events per PP Repeat Unit. High-*T* GPC data were obtained for neat PP pellets and the linear PP-*g*-ES/1, PP-*g*-ES/2, and PP-*g*-ES/3.[74] In order to draw a comparison that reflects chain scission that could occur during the purification process, we evaluated those samples that had been washed with acetone and annealed at 50 °C under vacuum for 48 h and which showed larger reductions in η_0 than samples that had been annealed at room temperature for 96 h. Samples were dissolved in trichlorobenzene and tested at 145 °C; data from a triple detection method were used in this paper. (It is important to note that data associated with triple detection provided the worst case scenario for percent reductions in MW as compared to data from other detection methods.[75]) Average MW values, as well as percent reduction in number-average MW (M_n) and percent reduction in M_w, for these samples are presented in Table 2. The percent reductions in M_w, as determined from high-*T* GPC, are in good agreement with those determined from rheology (see Table 2). As expected, the percent reduction in M_w is greater than the corresponding percent reduction in M_n for each sample. This is because the probability that a chain undergoes scission increases as the chain length increases, thereby resulting in a greater reduction in M_w than M_n.

The average number of scission events per chain can be determined from the M_n data:[12]

$$z_c = [M_{n,0}/M_{n,f}] - 1 \quad (3)$$

where $M_{n,0}$ is the initial M_n, and $M_{n,f}$ is the final M_n after scission (and purification). Based on eq 3, z_c = 0.10 scission events per chain for PP-*g*-ES/1, i.e., for every 100 original PP chains, there were 10 scission events. If we assume that each scission event resulted in the formation of a radical at each chain end,[76] then we can expect a total of 20 benzoates to be grafted onto 110 PP chains. However, on the basis of the 104 900 g/mol M_n and 0.08 mol % grafting degree for PP-*g*-ES/1, we determine that ∼2 benzoates are grafted per chain. Thus, for 110 chains, PP-*g*-ES/1 contains ∼220 grafted benzoates, a factor of 11 more than the number of chain ends created. This indicates that the vast majority of benzoates are grafted along the PP backbone and not only at chain ends, that little of the benzoate grafting is due to reaction of benzoyloxy radicals with PP radicals formed by chain scission accompanying SSSP, and that the limit for grafting yield during SSSP (as defined by eq 2) is at most slightly above 100%.[76] This also provides further proof that during SSSP PP macroradicals are less likely to undergo β-scission, thus allowing for benzoate functionalization along the PP backbone. Using similar analyses, z_c and the number of benzoates per chain for PP-*g*-ES/2 and PP-*g*-ES/3 were determined and are shown Table 2. For both PP-*g*-ES/2 and PP-*g*-ES/3, the number of benzoates grafted onto the PP chain vastly exceeds what would have been expected if the benzoyloxy radical only terminated with PP macroradicals produced as a result of chain scission accompanying SSSP.

With z_c = 0.10 for PP-*g*-ES/1 and PP-*g*-ES/2 and noting that $M_{n,0}$ = 115 000 g/mol for the neat PP starting material, we determine that one scission event happens every 26 100 repeat units. A similar calculation indicates that one scission event happens every 12 400 repeat units in the synthesis (and purification) of PP-*g*-ES/3. For PP-*g*-ES syntheses by Saule et al.[35] at 160 °C in inert environments and resulting in 30−40% grafting yields, we calculate that there was one scission event per 1000−2000 repeat units. Thus, PP-*g*-ES synthesis by SSSP results not only in higher grafting yield (62−87% for PP-*g*-ES/1, PP-*g*-ES/2, and PP-*g*-ES/3) but also in a factor of ∼10 lower frequency of scission events as compared to PP-*g*-ES prepared by Saule et al.[35]

For the PP-*g*-ES sample with only 0.02 mol % ester functional group synthesized by Assoun et al.[37] by melt processing in an inert environment, we calculate that one scission event occurred for every 11 800 repeat units. In comparison with PP-*g*-ES/1 (prepared with similar peroxide feed composition of ∼0.1 mol %), the PP-*g*-ES prepared by Assoun et al.[37] showed not only a much lower grafting degree as compared to its SSSP counterpart (0.08 mol % grafting degree and one scission event per 26 100 repeat units) but also a factor of 2 higher frequency of chain scission. Thus, relative to postpolymerization synthesis by melt processing, PP-*g*-ES synthesis by SSSP results in enhanced grafting degree and yield and in a major reduction in the frequency of chain scission events per repeat unit, which in turn causes MW reduction.

Given our recent success in synthesizing maleic anhydride modified PP (PP-*g*-MA) via SSSP of PP in the presence of MA and azobis(isobutyronitrile) (AIBN) as radical initiator,[12] it is also important to compare the level of chain scission events that occur during the SSSP syntheses of PP-*g*-ES and PP-*g*-MA. For a PP-*g*-MA sample with 0.21 mol % MA functionalization, high-*T* GPC analysis revealed that one scission event occurred for every 24 500 repeat units,[12] which is approximately one-half the level of chain scission in PP-*g*-ES/3 (one per 12 400 repeat units) with 0.18 mol % ES functionalization. The increase in the frequency of scission events for PP-*g*-ES/3 as compared to its PP-*g*-MA counterpart (both synthesized via SSSP) can be attributed to the fact that BPO radicals participate in chain transfer with PP to a much greater extent than radicals from AIBN (the radical initiator used to synthesized PP-*g*-MA via SSSP).[77] Nevertheless, it is evident that polar functionalization of PP via SSSP affords us the ability to suppress the frequency of chain scission events (and hence suppress MW reduction) by taking advantage of the low-*T* processing conditions associated with SSSP.

dx.doi.org/10.1021/ma401628u | Macromolecules 2013, 46, 7834−7844

Physical and Mechanical Properties. Table 1 shows the percent crystallinity for PP-*g*-ES samples made by SSSP. Percent crystallinity (χ_{crys}) was determined using eq 4:

$$\chi_{crys} = (\Delta H_f/\Delta H^\circ_f) \times 100\% \quad (4)$$

where ΔH_f is the sample enthalpy of fusion and ΔH°_f is enthalpy of fusion for 100% crystalline PP (ΔH°_f = 207.1 J/g[78]). Within experimental error, we observe that SSSP of neat PP does not affect crystallinity. For PP-*g*-ES samples, there are only slight decreases in crystallinity relative to neat as-received PP, from 45% to 40−42%. This behavior can be explained by the fact that the bulky benzoate groups grafted onto the PP backbone (and possibly the presence of PP branches) disrupt crystal formation.

Table 1 also compares Young's modulus (E) and yield strength (σ_y) values of neat PP before and after SSSP with those of PP-*g*-ES samples. Within error, SSSP of neat PP had no effect on E and σ_y, consistent with the fact that the MW and crystallinity of neat PP before and after SSSP were little changed or identical within error. The grafting of PP with 0.08−0.30 mol % benzoate by SSSP results in no change E within error from the value for neat as-received PP and, at most, only a ∼10% reduction in σ_y. However, with 0.41 mol % ester functionalization (sample PP-*g*-ES/5), there is a slightly less than 15% decrease in E and a 20% decrease in σ_y relative to neat as-received PP, both outside experimental error. These small reductions may be expected as tensile properties of PP are closely linked to MW and crystallinity, both of which decrease slightly with benzoate grafting and are lowest for PP-*g*-ES/5.[79]

Interfacial Property Modification: Contact Angle Characterization. In order to verify the improved wettability and polarity of PP-*g*-ES samples as compared to neat as-received PP, contact angles were measured for sessile drops of deionized water placed on the surfaces of smooth neat PP and PP-*g*-ES films (see Figure 5). The contact angle decreases smoothly with increasing level of ester grafting, which is consistent with the notion that functionalized PP will have improved interfacial adhesion with more polar materials as compared to the parent PP from which it was synthesized.[80,81] In contrast, the contact angle of neat PP after SSSP remains unchanged, within error, as compared to the neat, as-received PP. Thus, the polarity of neat PP is unaffected by SSSP processing; this is consistent with our observation of the absence of ketonization or carboxylic acid formation from any radical stabilization by atmospheric oxygen.[54] These results provide further confirmation of the ability of SSSP to achieve direct ester functionalization PP using BPO and that PP interfacial properties can be easily tuned via ester functionalization by SSSP.

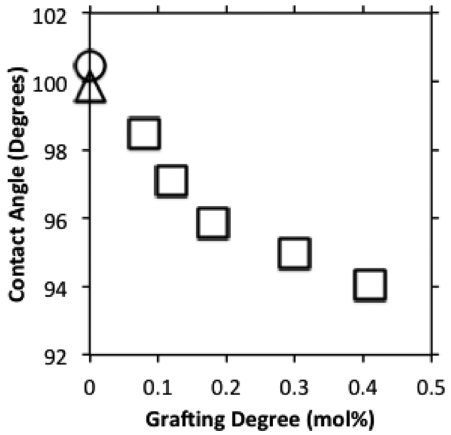

Figure 5. Contact angle measurements of neat PP pellets as received (○), neat PP after pulverization (△), and PP-*g*-ES samples synthesized via SSSP with varying degrees of ester functionalization (□).

Reactivity of PP-*g*-ES with Pyr-AA. Functionalized polyolefins are often used commercially as reactive compatibilizers for immiscible blends.[17,82−85] As further proof of functionalization and to demonstrate reactivity of the PP-*g*-ES, we investigated the reactivity of the PP-*g*-ES synthesized by SSSP with Pyr-AA. Under the conditions of reaction, transesterification between PP-*g*-ES and Pyr-AA is expected, resulting in a covalent attachment of pyrenyl moieties to the PP backbone.[86] The presence of pyrenyl units covalently attached to PP is easily confirmed by fluorescence spectroscopy.[87,88]

Figure 6 compares the fluorescence spectra of a solution of 0.3 g/L Pyr-AA in xylene and a 2.0 g/L PP-*g*-ES/5 solution in xylene after reaction with Pyr-AA (followed by six cycles of dissolution/precipitation to remove any unreacted Pyr-AA). The spectrum for PP-*g*-ES/5 shows slight shifts in pyrenyl emission peak wavelengths and structure as compared to that for Pyr-AA; these shifts have been observed in other studies and are associated with modification of photophysical responses (e.g., the polarization, intensity, and energy of the fluorescence transitions) caused by the nature of the chromophore attachment to the polymer backbone.[88−90] Nonetheless, the fluorescence observed for PP-*g*-ES/5 after reaction with Pyr-AA provides further proof of direct functionalization of PP with benzoates using BPO only and of the potential utility of PP-*g*-ES as reactive compatibilizer in polymer blends. Control studies carried out on neat PP and PP-*g*-ES/4MM (synthesized via melt processing), using the same reaction and purification protocol as for PP-*g*-ES/5, resulted in no fluorescence.

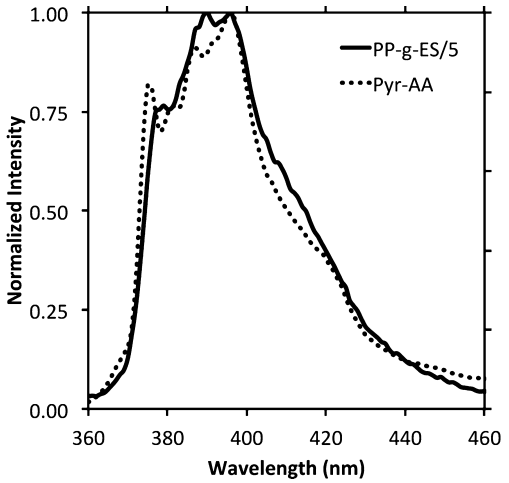

Figure 6. Fluorescence spectra of 0.3 g/L solution of Pyr-MeNH$_2$ in xylene at 100 °C (dotted curve) and 2 g/L solution PP-*g*-ES/5 in xylene at 100 °C after first being reacted with Pyr-AA and then purified six times by dissolution and precipitation to remove unreacted Pyr-AA. (Both spectra have had emission intensity normalized to unity at the peak emission wavelength.)

dx.doi.org/10.1021/ma401628u | *Macromolecules* 2013, 46, 7834−7844

CONCLUSION

This study demonstrated a novel method of achieving direct ester functionalization of PP using BPO, a symmetric organic peroxide; during SSSP, functionalization is made possible by both thermal and mechanochemical decomposition of BPO at the near-ambient processing T. At these T conditions, the extent of decarboxylation of the benzoyloxy radicals formed during BPO decomposition is significantly decreased, allowing for effective functionalization of PP with ester functional groups (i.e., benzoates), resulting in grafting yields of 36−87%. Contrary to the functionalization realized by SSSP processing, the high-T conditions associated with melt processing result in no grafting for a similar system of PP and BPO because of high extents of decarboxylation. Thus, SSSP provides a new platform of chemistries, which are not attainable via melt processing, for direct functionalization of PP with benzoates.

In addition to achieving PP functionalization with benzoates using BPO, we also demonstrated that this functionalization can be attained with limited reductions in M_n and M_w; for PP-*g*-ES with 0.18 mol % benzoate groups, only one chain scission event happens for every 12 400 repeat units, resulting in a 17% reduction in M_n and a 36% reduction in M_w. These moderate MW reductions are achieved because of the low processing T employed during SSSP. Under the high T conditions utilized with melt processing, the extent of β-scission, the primary cause of MW reduction, is high. By processing via SSSP, we strongly suppress the extent of β-scission and thus suppress MW reduction that could accompany functionalization.

Using contact angle measurements and based on a transesterification reaction with Pyr-AA, we provided further proof of successful polar functionalization of PP. We showed that the contact angle of a droplet of deionized water decreased with grafting degree, proving an increase in polarity for PP-*g*-ES samples relative to the neat, parent PP. Transesterification of PP-*g*-ES with a fluorescent chromophore was used to demonstrate potential in reactive compatibilization. Finally, the little to no reduction in crystallinity coupled with moderate MW reductions resulted in PP-*g*-ES samples with little to no losses in mechanical and physical properties relative to the neat parent PP. Together, these results confirm that SSSP can be used to achieve direct ester functionalization of PP to high grafting yields and without the use of a polar monomer.[29,91]

ASSOCIATED CONTENT

Supporting Information

Additional rheology data demonstrating the absence of zero shear rate regimes of some PP-*g*-ES samples, an indication of branching, and high-T GPC chromatograms of some PP-*g*-ES samples. This material is available free of charge via the Internet at http://pubs.acs.org.

AUTHOR INFORMATION

Corresponding Author

*E-mail j-torkelson@northwestern.edu (J.M.T.).

Notes

The authors declare no competing financial interest.

ACKNOWLEDGMENTS

We acknowledge support from a 3M Graduate Fellowship (to M.F.D.), the Initiative for Sustainability and Energy at Northwestern (ISEN), and Northwestern University. This study used Central Facilities supported by the MRSEC program of the National Science Foundation at the Northwestern University Materials Research Science and Engineering Center. High-T GPC was performed at the Polymer Characterization Lab at the University of Tennessee.

REFERENCES

(1) Chung, T. C. *Prog. Polym. Sci.* **2002**, *27*, 39−85.
(2) Bae, C.; Hartwig, J. F.; Boaen Harris, N. K.; Long, R. O.; Anderson, K. S.; Hillmyer, M. A. *J. Am. Chem. Soc.* **2005**, *127*, 767−76.
(3) Iizuka, Y.; Sugiyama, J.; Hagihara, H. *Macromolecules* **2009**, *42*, 2321−2323.
(4) Pesetskii, S. S.; Jurkowski, B.; Makarenko, O. A. *J. Appl. Polym. Sci.* **2002**, *86*, 64−72.
(5) Chmela, S.; Fiedlerova, A.; Janigova, I.; Novak, I.; Borsig, E. *J. Appl. Polym. Sci.* **2011**, *119*, 2750−2758.
(6) Minoura, Y.; Ueda, M.; Mizunuma, S.; Oba, M. *J. Appl. Polym. Sci.* **1969**, *13*, 1625−1640.
(7) Shi, D.; Yang, J.; Yao, Z.; Wang, Y.; Huang, H.; Jing, W.; Yin, J.; Costa, G. *Polymer* **2001**, *42*, 5549−5557.
(8) Ni, Q.-L.; Fan, J.-Q.; Niu, H.; Dong, J.-Y. *J. Appl. Polym. Sci.* **2011**, *121*, 2512−2517.
(9) Ho, R. M.; Su, A. C.; Wu, C. H.; Chen, S. I. *Polymer* **1993**, *34*, 3264−3269.
(10) De Roover, B.; Sclavons, M.; Carlier, V.; Devaux, J.; Legras, R.; Momtaz, A. *J. Polym. Sci., Part A: Polym. Chem.* **1995**, *33*, 829−842.
(11) Zhang, M.; Colby, R. H.; Milner, S. T.; Chung, T. C. M.; Huang, T.; DeGroot, A. W. *Macromolecules* **2013**, *46*, 4313−4323.
(12) Diop, M. F.; Torkelson, J. M. *Polymer* **2013**, *54*, 4143−4154.
(13) Wang, Z. M.; Hong, H.; Chung, T. C. *Macromolecules* **2005**, *38*, 8966−8970.
(14) Kobayashi, S.; Kim, H.; Macosko, C. W.; Hillmyer, M. A. *Polym. Chem.* **2013**, *4*, 1193−1198.
(15) Nakamura, A.; Ito, S.; Nozaki, K. *Chem. Rev.* **2009**, *109*, 5215−5244.
(16) Kitayama, N.; Keskkula, H.; Paul, D. R. *Polymer* **2000**, *41*, 8041−8052.
(17) Roeder, J.; Oliveira, R. V. B.; Goncalves, M. C.; Soldi, V.; Pires, A. T. N. *Polym. Test.* **2002**, *21*, 815−821.
(18) Li, Y.; Shimizu, H. *Eur. Polym. J.* **2009**, *45*, 738−746.
(19) Bullions, T. A.; Gillespie, R. A.; Price-O'Brien, J.; Loos, A. C. *J. Appl. Polym. Sci.* **2004**, *92*, 3771−3783.
(20) Arbelaiz, A.; Fernandez, G.; Cantero, G.; Llano-Ponte, R.; Valea, A.; Mondragon, I. *Composites, Part A* **2005**, *36*, 1637−1644.
(21) Okada, A.; Usuki, A. *Macromol. Mater. Eng.* **2006**, *291*, 1449−1476.
(22) Martín, Z.; Jimenez, I.; Gomez-Fatou, M. A.; West, M.; Hitchcock, A. P. *Macromolecules* **2011**, *44*, 2179−2189.
(23) Sánchez-Valdes, S.; Ramírez-Vargas, E.; Ibarra-Alonso, M. C.; Ramos de Valle, L. F.; Méndez-Nonell, J.; Medellín-Rodríguez, F. J.; Martínez-Colunga, J. G.; Vazquez-Rodriguez, S.; Betancourt-Galindo, R. *Composites, Part B* **2012**, *43*, 497−502.
(24) Rätzsch, M.; Arnold, M.; Borsig, E.; Bucka, H.; Reichelt, N. *Prog. Polym. Sci.* **2002**, *27*, 1195−1282.
(25) Coiai, S.; Passaglia, E.; Aglietto, M.; Ciardelli, F. *Macromolecules* **2004**, *37*, 8414−8423.
(26) Passaglia, E.; Coiai, S.; Augier, S. *Prog. Polym. Sci.* **2009**, *34*, 911−947.
(27) Gaylord, N. G.; Mishra, M. K. *J. Polym. Sci., Lett. Ed.* **1983**, *21*, 23−30.
(28) Gloor, P. E.; Tang, Y.; Kostanska, A. E.; Hamielec, A. E. *Polymer* **1994**, *35*, 1012−1030.
(29) Boaen, N. K.; Hillmyer, M. A. *Chem. Soc. Rev.* **2005**, *34*, 267−275.
(30) DeNicola, A. J. J.; Wei-Berk, C. C. H.; Hogt, A. H.; Jelenic, J.; Meijer, J. Modification of (co)polymers with unsaturated peroxyacids. US Patent 5,447,985, Sept 5, 1995.
(31) Navarre, S.; Maillard, B. *J. Polym. Sci., Part A: Polym. Chem.* **2000**, *38*, 2957−2963.

(32) Navarre, S.; Degueil, M.; Maillard, B. *Polymer* **2001**, *42*, 4509−4516.
(33) Navarre, S.; Saule, M.; Maillard, B. *J. Appl. Polym. Sci.* **2003**, *87*, 699−707.
(34) Saule, M.; Navarre, S.; Babot, O.; Maslow, W.; Vertommen, L.; Maillard, B. *Macromolecules* **2003**, *36*, 7469−7476.
(35) Saule, M.; Moine, L.; Degueil-Castaing, M.; Maillard, B. *Macromolecules* **2005**, *38*, 77−85.
(36) Anbarasan, R.; Babout, O.; Dequil, M.; Maillard, B. *J. Appl. Polym. Sci.* **2005**, *97*, 761−765.
(37) Assoun, L.; Manning, S. C.; Moore, R. B. *Polymer* **1998**, *39*, 2571−2577.
(38) Sheppard, C. S.; Kamath, V. R. *Polym. Eng. Sci.* **1979**, *19*, 597−606.
(39) Initiators, Free-radical. *Kirk-Othmer Encyclopedia of Chemical Technology*, 5th ed.; Wiley: New York, 2001; Vol. *14*.
(40) Chateauneuf, J.; Lusztyk, J.; Ingold, K. U. *J. Am. Chem. Soc.* **1988**, *110*, 2886−2893.
(41) Brunner, P. J.; Torkelson, J. M. *Plast. Eng.* **2012**, *68* (9), 28−34.
(42) Brunner, P. J.; Clark, J. T.; Torkelson, J. M.; Wakabayashi, K. *Polym. Eng. Sci.* **2012**, *52*, 1555−1564.
(43) Furgiuele, N.; Lebovitz, A. H.; Khait, K.; Torkelson, J. M. *Macromolecules* **2000**, *33*, 225−228.
(44) Lebovitz, A. H.; Khait, K.; Torkelson, J. M. *Macromolecules* **2002**, *35*, 8672−8675.
(45) Tao, Y.; Kim, J.; Torkelson, J. M. *Polymer* **2006**, *47*, 6773−6781.
(46) Lebovitz, A. H.; Khait, K.; Torkelson, J. M. *Macromolecules* **2002**, *35*, 9716−9722.
(47) Masuda, J.; Torkelson, J. M. *Macromolecules* **2008**, *41*, 5974−5977.
(48) Wakabayashi, K.; Pierre, C.; Dikin, D. A.; Ruoff, R. S.; Ramanathan, T.; Brinson, L. C.; Torkelson, J. M. *Macromolecules* **2008**, *41*, 1905−1908.
(49) Wakabayashi, K.; Brunner, P. J.; Masuda, J.; Hewlett, S. A.; Torkelson, J. M. *Polymer* **2010**, *51*, 5525−5531.
(50) Iyer, K. A.; Torkelson, J. M. *Polym. Compos.* **2013**, *34*, 1211−1221.
(51) Jiang, X.; Drzal, L. T. *J. Appl. Polym. Sci.* **2012**, *124*, 525−535.
(52) Macosko, C. W.; Maric, M. *Polym. Eng. Sci.* **2001**, *41*, 118−130.
(53) Smith, B. *Infrared Spectral Interpretation: A Systematic Approach*, 1st ed.; CRC Press: Boca Raton, FL, 1998.
(54) Wilhelm, C.; Gardette, J. *J. Appl. Polym. Sci.* **1994**, *51*, 1411−1420.
(55) O'Neil, G. A.; Torkelson, J. M. *Macromolecules* **1999**, *32*, 411−422.
(56) From the studies by Saule et al. in refs 34 and 35, inferences of grafting degrees could not be made because the necessary information was not provided in those references.
(57) Kaupp, G. *CrystEngComm* **2009**, *11*, 380−403.
(58) Caruso, M. M.; Davis, D. A.; Shen, Q.; Odom, S. A.; Sottos, N. R.; White, S. R.; Moore, J. S. *Chem. Rev.* **2009**, *109*, 5755−5798.
(59) Brantley, J. N.; Wiggins, K. M.; Bielawski, C. W. *Polym. Int.* **2013**, *62*, 2−12.
(60) Liu, Y.; Wang, Q. *Polym. J.* **2002**, *34*, 132−137.
(61) At 200 °C, 2 s is required to achieve 99.99% decomposition of BPO (see ref 55). This extremely high rate of decomposition of BPO under melt processing conditions, followed by subsequent formation of inert molecules, makes BPO inappropriate for the formation of PP macroradicals during melt processing.
(62) Barnett, B.; Vaughan, W. *J. Phys. Chem.* **1947**, *51*, 942−955.
(63) Dickens, B. *J. Polym. Sci., Polym. Chem.* **1982**, *20*, 1169−1183.
(64) Carson, A. S.; Laye, P. G.; Morris, H. *J. Chem. Thermodyn.* **1975**, *7*, 993−996.
(65) Langmuir, I. *Phys. Rev.* **1913**, *2*, 329−342.
(66) Félix-Rivera, H.; Ramírez-Cedeño, M. L.; Sánchez-Cuprill, R. A.; Hernández-Rivera, S. P. *Thermochim. Acta* **2011**, *514*, 37−43.
(67) Sublimation and decomposition occur simultaneously during the annealing process; the rate of decomposition increases with increasing T (see ref 55) while that of sublimation decreases with increasing T (see refs 62−64). Because BPO decomposition during subsequent melt processing could lead to additional MW reduction, its removal by sublimation is preferred in cases where MW reduction must be minimized. Approximations of the time required to remove excess BPO by sublimation can be determined using the equation for the rate of sublimation (see refs 64 and 65): $dm/dt = P\alpha[M/(2\pi RT)]^{1/2}$, where dm/dt is change in mass per unit time per unit area, P is the vapor pressure of the solid, α is a vaporization coefficient (α = 1 in vacuum, see ref 66), M is molecular weight, R is the ideal gas constant, and T is absolute temperature. Thus, one can control the relative extents of sublimation and decomposition by varying annealing T and time. For example, by decreasing the annealing T, sublimation will be become the dominant of the two process though more time will be required to remove the same amount of BPO.
(68) Bird, B. R.; Curtiss, C. F.; Armstrong, R. C.; Hassager, O. *Dynamics of Polymeric Liquids*, 2nd ed.; Wiley: New York, 1987; p 437.
(69) Cross, M. M. *J. Colloid Sci.* **1965**, *20*, 417−437.
(70) Bremner, T.; Rudin, A.; Cook, D. G. *J. Appl. Polym. Sci.* **1990**, *41*, 1617−1627.
(71) Fujiyama, M.; Kitajima, Y.; Inata, H. *J. Appl. Polym. Sci.* **2002**, *84*, 2128−2141.
(72) Graessley, W. W.; Struglinski, M. J. *Macromolecules* **1986**, *19*, 1754−1760.
(73) Ferry, J. D. *Viscoelastic Properties of Polymers*; Wiley: New York, 1980; p 641.
(74) Molecular weight averages were evaluated by high-T GPC (at 145 °C with trichlorobenzene as eluent and triple detection) at the Polymer Characterization Lab at the University of Tennessee, Knoxville, TN 37996.
(75) Using trichlorobenzene as solvent, GPC samples were run at 145 °C and analyzed with light scattering, triple detection, and universal calibration. We used the triple detection data in the analysis described in the Results and Discussion section. The standard deviation of MW data from universal calibration, light scattering, and triple detection is 19 000 g/mol for M_n and 17 000 g/mol for M_w. Percent reductions in M_n and M_w were highest for triple detection data for all PP-*g*-ES samples. For light scattering the following values were obtained: PP-*g*-ES/1 (9 and 22% reductions in M_n and M_w, respectively), PP-*g*-ES/2 (3 and 23% reductions in M_n and M_w, respectively), and PP-*g*-ES/3 (14 and 34% reductions in M_n and M_w, respectively). For universal calibration the following values were obtained: PP-*g*-ES/1 (10 and 16% reductions in M_n and M_w, respectively), PP-g-ES/2 (12 and 25% reductions in M_n and M_w, respectively), and PP-g-ES/3 (13 and 29% reductions in M_n and M_w, respectively). Averaged across all three detection methods, the following M_n and M_w values were obtained for neat PP pellets (M_n = 142 200 g/mol and M_w = 585 100 g/mol) and resulted in percent reductions in M_n and M_w of 6−18% and 21−33%, respectively, for PP-*g*-ES samples.
(76) The stoichiometric analysis used here is based on the worst possible scenario, i.e., two PP macroradicals formed from each chain scission. When chain scission occurs as a result of β-scission, only one PP macroradical will be formed; thus, fewer PP radicals will be produced, and this requires that more benzoates be attached to each PP chain. This outcome provides even greater evidence in favor of benzoate units attached along the PP backbone.
(77) Zweifel, H. *Stabilization of Polymeric Materials*, 1st ed.; Springer: Berlin, 1998.
(78) Bu, H.-S.; Cheng, S. Z. D.; Wunderlich, B. *Makromol. Chem., Rapid Commun.* **1988**, *9*, 75−77.
(79) The yield strength of polyolefins is also linked to molecular weight. However, since PP-*g*-ES/5 shows evidence of branching from rheology data, we are unable to characterize the molecular weight (average or distribution) of this sample, although we expect it to be lowest of the SSSP samples.
(80) Balart, J.; Fombuena, V.; Balart, R.; Espana, J. M.; Navarro, R.; Fenollar, O. *J. Appl. Polym. Sci.* **2010**, *116*, 3256−3264.
(81) Chen, H. J.; Zhu, Y. F.; Zhang, Y.; Xu, J. R. *J. Polym. Res.* **2007**, *14*, 489−496.

(82) Manning, S. C.; Moore, R. B. *Polym. Eng. Sci.* **1999**, *39*, 1921−1929.
(83) Moad, G. *Prog. Polym. Sci.* **1999**, *24*, 81−142.
(84) Pruthtikul, R.; Liewchirakorn, P. *Adv. Mater. Res.* **2010**, *93*−*94*, 451−454.
(85) Keskkula, H.; Gonzalex-Montiel, A.; Paul, D. R. *Polymer* **1995**, *36*, 4605−4620.
(86) Otera, J.; Nishikido, J. *Esterification: Methods, Reactions, and Applications*, 2nd ed.; Wiley-VCH: Weinheim, 2010.
(87) Kim, S. D.; Torkelson, J. M. *Macromolecules* **2002**, *35*, 5943−5952.
(88) Kim, S.; Roth, C. B.; Torkelson, J. M. *J. Polym. Sci., Part B: Polym. Phys.* **2008**, *46*, 2754−2764.
(89) Duhamel, J. *Molecular Interfacial Phenomena of Polymers and Biopolymers*; Chen, P., Ed.; Woodhead Publishing: Cambridge, England, 2005; pp 214−248.
(90) Berlman, I. B. *Handbook of Fluorescence Spectra of Aromatic Molecules*; Academic Press: New York, 1971; p 48.
(91) Diop, J. M.; Torkelson, J. M.; Carbonyl Functionalization of Polypropylene via Solid-State Shear Pulverization. US Provisional Patent filed on Sept 21, 2012.